

Simulation of ion-track ranges in uranium oxide

Byoungseon Jeon^{a,*}, Mark Asta^{b,c}, Steven M. Valone^d, Niels Grønbech-Jensen^a

^a Department of Applied Science, University of California, Davis, CA 95616, United States

^b Department of Materials Science and Engineering, University of California, Berkeley, CA 94720, United States

^c Department of Chemical Engineering and Materials Science, University of California, Davis, CA 95616, United States

^d Materials Science and Technology Division, Los Alamos National Laboratory, Los Alamos, NM 87544, United States

ARTICLE INFO

Article history:

Received 30 March 2010

Received in revised form 18 May 2010

Available online 9 June 2010

Keywords:

REED-MD

Ion-track range

Molecular dynamics

Nuclear fuel materials

Uranium oxide

ABSTRACT

Direct comparisons between statistically sound simulations of ion-tracks and published experimental measurements of range densities of iodine implants in uranium dioxide have been made with implant energies in the range of 100–800 keV. Our simulations are conducted with REED-MD (Rare Event Enhanced Domain-following Molecular Dynamics) in order to account for the materials structure in both single crystalline and polycrystalline samples. We find excellent agreement between REED-MD results and experiments for polycrystalline target materials.

© 2010 Elsevier B.V. All rights reserved.

1. Introduction

Ion irradiation of materials with subsequent analysis of associated dopant density distributions by, e.g., secondary ion mass spectroscopy (SIMS) is a powerful tool for understanding irradiation effects in materials [1]. Dopant implantation into crystalline target materials provides especially detailed information about effective ionic size, atomic force-field, interatomic interactions, particularly at close distances, and the role of dissipation by electronic excitations. This is due to the variety of typical interaction mechanisms reflected in the statistics of ion-trajectories which are influenced by a variety of processes ranging from direct atomic collisions, to propagation through open channels of a given crystal structure with relatively minor interactions with the surrounding environment. The analysis of sets of carefully prepared SIMS profiles from different selected ion implantation experiments can therefore provide a wealth of information and the validation of theoretical models, which, in turn, can be used to interpret other experimentally generated SIMS profiles. Such validated theoretical models can also be used to study the trajectory of energetic ions arising from radiation damage, or from fission events in nuclear fuels.

Simulating dopant density distributions due to ion implantation or radiation damage is naturally done with atomic representations, since the evolution of a trajectory is governed by its atomic scale interactions with the target material. However, conducting full molecular dynamics (MD) simulation has several issues in the

analysis of ion implantations. First, very high-energy ions with MeV kinetic energies can reach depths of up to several micrometers. This is especially true for relevant radiation effects in nuclear fuel materials, where fission products have energies in the 100 MeV range and α -decay of heavy elements results in recoils in the range of 100 keV. Thus, the simulated volume of material needs to include billions of atoms in a MD simulation scheme and this is not an easy task even with state-of-art supercomputers. Secondly, due to the very high initial ion energy, the necessary time step of a numerical integrator for advancing the simulation is so small that an unpractical number of time steps is needed in order to resolve the dynamics during high-energy atomic collisions. Third, experimental ion-range data is a statistical composite of a very large number of ion-trajectories that make up the resulting measured distributions. Thus, one needs to conduct enough ion track simulations for a statistically meaningful density profile of resting ions to be obtained, and the number of required simulations is more than several thousand. Finally, in addition to these computing cost and efficiency issues, the standard MD method does not account for electron coupling effects in inelastic collisions. This is a particularly important issue for energetic ions where the role of electron stopping is reported to be essential in implantation or radiation range analysis.

The conventional binary collision approximation (BCA) addresses at least the first two problems listed above, namely, the spatial and temporal scales. This is done by neglecting all ion-target interactions that are not primary to the ion; i.e., the ion only interacts with a single target atom at a time, and this interaction is modeled as a complete and instantaneous trajectory of a collision.

* Corresponding author.

E-mail address: bjeon@ucdavis.edu (B. Jeon).

While this approximation has proven to be extremely powerful for trajectories in materials where crystal structure and channeling can be neglected, such as very dense materials, disordered materials, or for ions that are large compared to the crystal channel dimensions [2], it has inherent deficiencies when channeling along characteristic crystal orientations becomes important.

Here we apply the rare event enhanced domain following molecular dynamics (REED-MD) technique, which is a hybrid method combining elements of the BCA and MD in order to provide physically relevant and computationally practical simulations of ion-implant density profiles in crystalline uranium dioxide. This algorithm, which has been described in detail elsewhere [3,4], simulates only a limited amount of the target material at any given time, while providing a full-symmetry description of the forces acting on the ion by the target material. Thus, tracks along channels are well accounted for. An additional feature of the algorithm is the rare event enhancement, which seeks to equalize the statistical accuracy across different magnitudes of ion density. Since typical density profiles have a dominant peak, where most statistical counts will apply, it follows that the rest of the simulated density profile will have progressively poorer statistical sampling as the density decreases. The algorithm compensates for this undesirable feature by simulating multiple clones with decreased weight of a moving ions if they contribute to low probability events. The algorithm is briefly described below and a complete description can be found in Refs. [3,4].

As is well known [5–7] and recently re-emphasized [8], the behavior of fission gas products can have a substantial impact on nuclear fuel performance and safety. After their formation during reactor operation, these species can diffuse to fuel-cladding interfaces and/or be released from the fuel. Either of these outcomes can have a deleterious effect on the reactor. Fission-gas release can also occur under various storage and disposal conditions. For these reasons it is valuable to be able to simulate the profiles of fission gas products as they are produced. Here, we apply our simulation methodology in comparison with published experiments of 100–800 keV iodine implants into UO_2 targets of different structural characteristics. Even though SIMS experiments and corresponding REED-MD calculations, which employ one dimensional ion implantations, are not exact reproductions of fission-product release, this comparison serves as a controlled validation of the physics models that can make predictions regarding more complex behavior relevant for fuel material evolution.

2. Implementation of REED-MD

The physics implemented into REED-MD for this application consists of different components. Atomic interactions are modeled by the universal screened core potential of Ziegler et al. (ZBL) [1], which objectively represents the effective screening of one atom in the presence of another. The computationally efficient functional form for the potential energy $V(r)$ of interaction between two atoms at a mutual distance r is given by the core repulsion between the nuclei along with a simple universal screening function

$$V(r) = \frac{e^2}{4\pi\epsilon_0 r} Z_1 Z_2 \phi_u, \quad (1)$$

where Z_i is the atomic number of atom i , ϵ_0 is the vacuum permittivity constant, and e is the unit of charge. The screening function is defined as

$$\phi_u = 0.18175e^{-3.1998x} + 0.50986e^{-0.94229x} + 0.28022e^{-0.4029x} + 0.028171e^{-0.20162x}, \quad (2)$$

where $x = r/a_U$ is a reduced pair distance, with a_U being the universal screening length

$$a_U = \frac{a_B}{Z_1^{0.23} + Z_2^{0.23}}, \quad (3)$$

where $a_B = \sqrt[3]{\frac{9\pi^2}{128} r_B}$, $r_B \approx 0.52918 \text{ \AA}$ being the Bohr radius. This interaction accounts neither for the electrostatic interactions in the ionic material nor for the details of chemical bonding. However, these particular interactions are negligible compared to the collision energy that determines the range profiles of high-energy ions. Thus, for this particular purpose, the universal ZBL interaction is sufficient since we do not concern ourselves with the low energy and near-equilibrium properties of the material.

Since MD does not take electronic degrees of freedom (DOF) into account in an explicit manner that allows for direct energy transfer from moving atoms to those DOF, we adopt two phenomenological mechanisms for energy dissipation. Firsov's inelastic collisions between atoms as described by Elteckov [9], is expressed as a function of the relative velocity between two atoms leading to the following expression for the interatomic force:

$$\mathbf{F}_{ij}(r) = \frac{0.7 \hbar}{\pi r_B^2} (\mathbf{v}_j - \mathbf{v}_i) \left[\frac{Z_i^2}{\left(1 + 0.8 \alpha Z_i^{1/3} r/a_B\right)^4} + \frac{Z_j^2}{\left(1 + 0.8(1 - \alpha) Z_j^{1/3} r/a_B\right)^4} \right], \quad (4)$$

$$\alpha = \left[1 + \left(\frac{Z_j}{Z_i} \right)^{1/6} \right]^{-1}, \quad (5)$$

where $Z_i \geq Z_j$.

Second, electronic stopping is employed using a slightly revised Brandt and Kitagawa formulation [10,11]. This phenomenological description connects drag on a moving atom with the atom type, the atom velocity, and the electron density which it is moving through. Thus, this term acts as local friction in the equation of motion for the atom of the form

$$\Delta E_e = \int_{\text{ion path}} (Z_1^*)^2 S(v_1, r_s(x)) dx, \quad (6)$$

where Z_1^* is the effective charge of the moving ion, and S is the stopping power of a unit charge. In the formulation of the stopping power, we employ an adjustable parameter r_s^0 , being a mean value of one-electron radius (Wigner-Seitz radius). This value can be determined empirically and allows the fine tuning of range profile. In this study, we used $r_s^0 = 1.20 \text{ \AA}$ for UO_2 tests. A detailed description of the formulation can be found in the Refs. [10,11].

Given that only short range interactions are included in the dynamics of a moving ion we adopt a *domain following strategy* [12], in which the ion of interest is modeled along with the unit cell it is currently in, as well as a buffer of one more unit cell layer surrounding the ion. For a standard stoichiometric fluorite UO_2 structure this becomes 325 simulated atoms with the moving ion interacting with target material up to a distance longer than one unit cell ($>5 \text{ \AA}$). All these atoms interact, but as the ion is moving out of one unit cell, and into the next, new unit cells are created ahead of the track, while material is discarded in its wake such that the ion always is located in the center of the $3 \times 3 \times 3$ unit cells. We thereby simulate the interaction of a moving ion with an infinite bulk target material. We construct the new unit cell material according to the thermally disordered fluorite structure at a given temperature, employing a Gaussian distribution of thermal atomic displacements.

MD simulation of an ion-track is modeled as prescribed above and with adaptive time step control according to both the kinetic energy of the ion and the potential energy of atomic collisions. One such simulation is initiated with an incident ion inserted with a random position within a unit cell of the target material, and an initial momentum according to the energy and direction of the ion-track. The trajectory is then followed until the ion slows to a given

threshold energy when the ion is defined to be at rest. The distribution of implanted ion depths is obtained by conducting many such simulations in order to provide a statistically representative ensemble of outcomes. However, the range density at the end of range is very low (rare), and we employ *Rare Event Enhancement* for better statistics, rather than increasing the number of initiated ions. The advantage of the rare event algorithm is that it selectively clones the system for ions that travel beyond a characteristic depth beyond which there is a small probability. Each clone evolves independently and with half the statistical weight of the original. A multiple of such cloning depths are applied such that each interval between these characteristic depths contain approximately the same statistical count of simulated ions as any other interval, thereby providing the same statistical accuracy regardless of the physical density of ions. This algorithm ensures uniform cpu consumption across the density distribution, regardless of the variation of the distribution. As a result, we can obtain good statistics at all scales of interest, which is especially important for fission product profiles with appreciable densities at large depths due to channeling. The two above-mentioned components represent the standard features of the REED-MD algorithm; more detailed descriptions can be found in Refs. [3,13,14]. Recently REED-MD has been parallelized with standard MPI (message passing interface) [4], and ions of up to ~ 100 MeV can be handled with adequate statistics when about 10^4 initial ions are simulated.

3. Modeling implant densities in polycrystalline samples

The structure of the material is one of several important parameters when studying ion range density profiles in crystalline targets. The orientation of the material relative to the incident direction of the ion beam is critical for the resulting profile. For polycrystalline targets, we must additionally be concerned with the typical size of the crystalline grains relative to the depth to which an ion travels as well as the width of the ion beam on the surface of the target. If the beam radius is small compared to the grain size, we may consider that only one grain orientation is relevant for the incoming ion. In this case one needs to have knowledge of the grain orientations. If the depth of the traveling ion is larger than the typical grain size, then one needs to insert characteristic disruptions in the target material orientation during the simulation of each individual ion-track. However, in the UO_2 SIMS experiments [8], it is reported that an ion radiation depth-profile (of hundreds of keV) extends to less than a micron, while the typical grain size of the polycrystalline samples is about $5\text{ }\mu\text{m}$. The applied beam size $150 \times 150\text{ }\mu\text{m}^2$ is, conversely, much larger than the grain size. Thus, the physical situation is as sketched in Fig. 1, where each ion-track simulation can be represented as an implant into a crystalline material, but with the crystal orientation randomly selected for that particular simulation (note that we are making the simplifying assumption that the sample is not textured and does not possess preferred relative grain orientations). The ensemble of such simulations is then assumed to be representative of the overall depth profile. We note that more sophisticated target material representations, in which grain boundaries are included in a simulation, could be adopted, but we would then need to know more about the characteristics of grain sizes from orientation imaging microscopy for instance. Given that this information is not provided for the experiments of interest, and that the ion range is significantly shorter than the reported typical grain size, we have conducted the simulations with the least amount of complexity.

Recent iodine implant experiments with SIMS analyses [8] include implant energies between 100 and 800 keV, and SIMS conducted after post-implant diffusion has been performed. We are not concerned with diffusion properties in this work, and we will

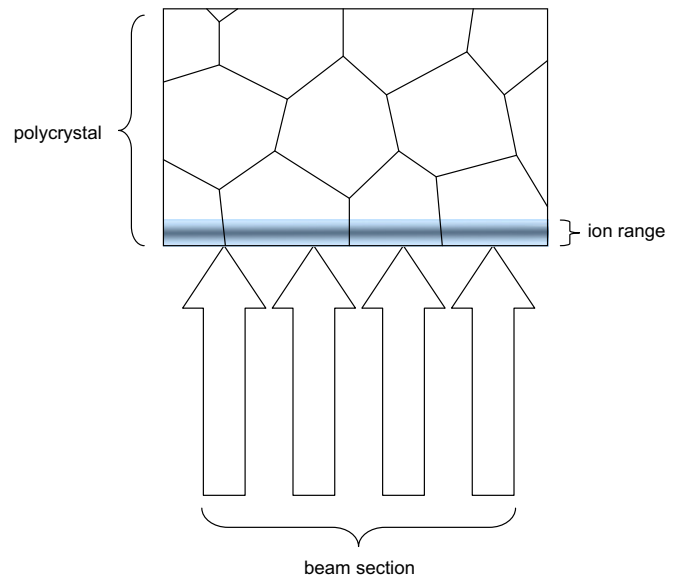


Fig. 1. Schematic diagram of the geometry associated with the ion implantation experiments for polycrystalline UO_2 .

therefore focus exclusively on the “as-implanted” SIMS results. These experiments can be directly simulated with the present approach.

First, for 100 keV iodine, we have conducted simulations of implant depth profiles for both single and polycrystalline targets, where the single crystalline simulations have been conducted such that the implant directions are aligned with the characteristic UO_2 fluorite crystal orientations [100], [110], and [111]. The results, obtained at 300 K, are summarized in Fig. 2, where the line-connected markers with error bars represent the four different simulation results. We observe clear distinctions between the different orientations, and we confirm that the deepest implants at this energy correspond to the orientations with the widest channels. It is noteworthy that the implant profiles for the polycrystalline sample are also distinct from the implants along the characteristic crystal orientations. This distribution is the one exhibiting the most initial atomic collisions, signified by the large short range peak in the distribution, yet with more channeling ions than what is found for the small channel-area direction [111]. This is consistent with a random orientation, since the initial peak represents all the off-axis implant events, while the few deep results are those where the implant direction has been aligned with one of the two large channel-area directions. The corresponding experimental data from Fig. 2 of Ref. [8], which is the result of measurements on polycrystalline target materials, is included as circular markers. The agreement between our orientationally averaged simulation results and the experimental data for the polycrystalline target materials is near-perfect for ranges below $0.2\text{ }\mu\text{m}$, which accounts for about two orders of magnitude in the density. After this distance, the experimental density is nearly flat, whereas the simulated profile continues to decay. This discrepancy can be due to the numerical representation of the polycrystalline target material. One may imagine that rapid diffusion may occur along grain boundaries; an effect that is not possible to model in our simulations. However, one may also speculate that the experimental density beyond $0.2\text{ }\mu\text{m}$ could reflect instrument resolution in the SIMS measurements. In any case, we consider the agreement convincing, and emphasize that any significant discrepancy occurs at densities two orders of magnitude below the peak value.

With this information, it is interesting to observe the comparable data for single-crystalline target materials shown in Ref. [8].

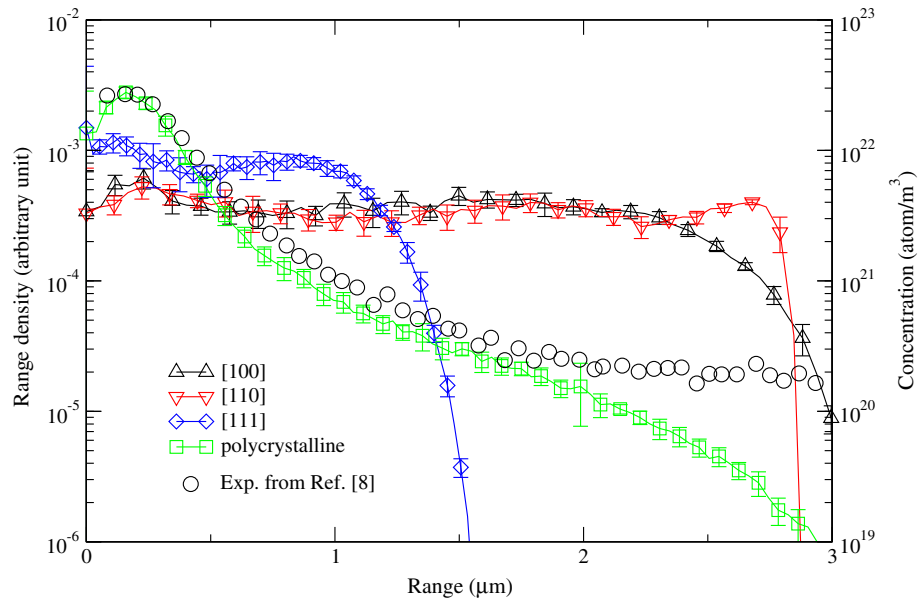


Fig. 2. Range density results of REED-MD for iodine 100 keV on UO_2 . Circular marks are the concentration data of iodine with polycrystalline UO_2 , sampled from Fig. 2 of Ref. [8].

This density profile looks very similar to that of the polycrystalline sample, and nothing like the simulated on-axis density profiles we report in Fig. 2. We cannot explain this discrepancy with any certainty, since we do not know the details of the materials processing or specific orientation of the surface in the single-crystal samples.

Next, we simulated the reported [8] 440 keV iodine implant into polycrystalline UO_2 . In addition to comparing the as-implanted SIMS profile to our REED-MD simulations, we have also included results of SRIM (stopping and range of ions in matter) [15] simulations in order to display the significance of channeling and structured target interactions guiding the moving ion. The results are displayed in Fig. 3, where the top plot shows the comparison between REED-MD and SRIM on a linear scale of density. It is obvious

that the primary, collisional peak in the distribution is well characterized by the BCA. There are only minor differences in the peak location, with the REED-MD results showing a slightly shorter depth. However, when looking at the data on a logarithmic scale of density, the lower part of Fig. 3, we see how the channeling tail of the profile is entirely absent in BCA. While this tail does not contain a large fraction of the implanted ions, it does show the extent of the implant range being several times larger than that simulated with BCA. Also on the lower plot of Fig. 3 is shown the experimental data as open circular markers. We again observe that the experiments support the profile obtained by REED-MD throughout three orders of magnitude of density, and we observe that the location of the primary peak in the distribution is also in agreement. As was the case for the results of 100 keV implants, discussed above, the

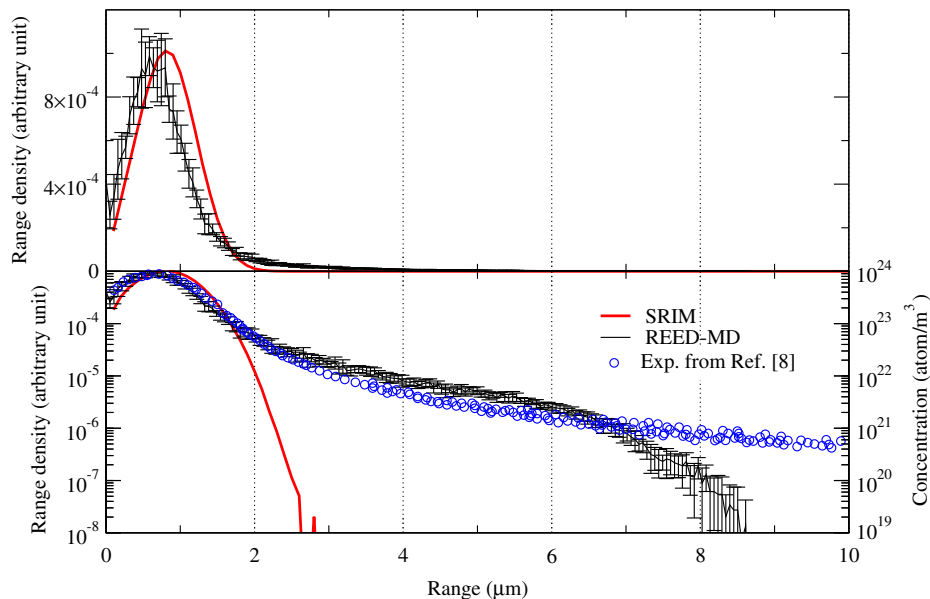


Fig. 3. Range density results of REED-MD and SRIM for iodine 440 keV on polycrystalline UO_2 . The top plot shows the results of SRIM and REED-MD on a linear scale while the bottom plot is on a log-scale. Circles on the bottom plot are iodine concentration data, sampled from Fig. 12 of Ref. [8].

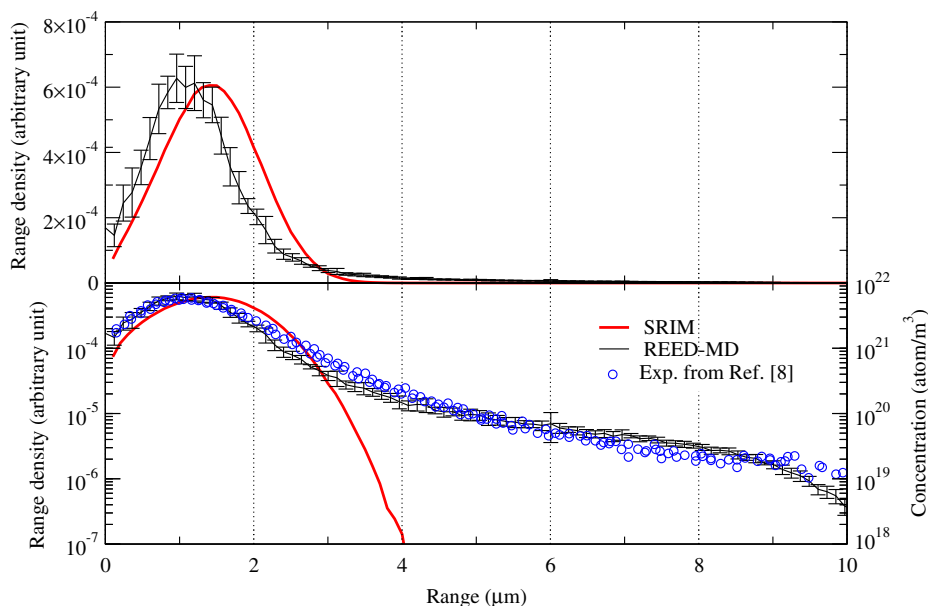


Fig. 4. Range density results of REED-MD and SRIM for iodine 800 keV on polycrystalline UO_2 . The top plot shows the results of SRIM and REED-MD on a linear scale while the bottom plot is on a log-scale. Circles on the bottom plot are iodine concentration data, sampled from Fig. 1 of Ref. [8].

longer tail of the experimental distribution may be due to either the noise level in the SIMS profile, high dose effects, or some fast diffusion along grain boundaries during the time frame of implantation.

Finally, we compare REED-MD with SRIM and the reported SIMS data for 800 keV iodine into polycrystalline samples. The results are shown in Fig. 4, and the observations are very similar to those for the 440 keV implants discussed above. SRIM and REED-MD give similar primary peaks of the distribution, but the BCA cannot adequately account for the extended tail of the distribution. The REED-MD result is validated by the experiments, both in the location of the primary peak and the extent of the long tail of the distribution, which agree for the entire range of data that is available.

We notice that the primary peak in the density profiles for 440 and 800 keV implants show that SRIM produces a peak location slightly deeper than that predicted by REED-MD. We also notice that the REED-MD depth seems to agree better with the experimental SIMS profile. Observing the two figures we conclude that this difference between REED-MD and SRIM measured relative to the peak depth is the same for 440 and 800 keV. While this shift naturally has its origin in the approximations of BCA compared to the more detailed dynamics modeled in REED-MD, it is not a simple task to identify exactly what is the cause since the resulting depth profile is a complex convolution of all interactions in the two approaches.

We also notice that the more detailed modeling approach applied in REED-MD is computationally costly compared to SRIM; although REED-MD is significantly more efficient than the (prohibitively expensive) full MD. While different systems and parameters show different comparisons between the two methods, one comparison of illustration is the 800 keV implant into UO_2 . For 10^6 simulated ions, SRIM required a day on a single 800 MHz desktop PC (Pentium III). In contrast, REED-MD required 12–16 h for 10,000 initial ions with eight cloning depths, using 16 threads of 2.93 GHz Xeon workstations. A direct comparison between timings is not meaningful since the rare event enhancement integral to obtaining sufficient statistics in REED-MD is not included in SRIM, but it is evident that SRIM is computationally more efficient, as it should be with the binary collision approximation.

4. Discussion and conclusion

We have provided direct comparisons between published experimental SIMS data for high-energy iodine implants into polycrystalline uranium-dioxide samples and comparable REED-MD simulations. The comparisons for all three reported energies are encouraging and provide validation of the modeling approach as a predictive tool for studying ion ranges in oxide nuclear fuel materials. The observed discrepancies for polycrystalline samples are minor, and only occur at the far range of the distributions where many plausible origins of discrepancies can be imagined. These include fast diffusion along grain boundaries during the time of implantation, and the possible instrument resolution limits in the SIMS measurements.

Our simulations are of specific importance for modeling the results of secondary ion mass spectrometry measurements. In a more general sense though, the present investigation shows that accurate implantation profiles may be simulated. This ability opens the possibility of using REED-MD simulations to aid in evaluating new fuel materials. Further validation of the modeling parameters can benefit from detailed experiments of well characterized on-axis implantations, since Fig. 2 illustrates the sensitivity of the range profiles as a function of implant direction.

Acknowledgments

This work was supported by the US Department of Energy Nuclear Energy Research Initiative for Consortia (NERI-C) contract number DR-FG07-071D14893, by the Materials Design Institute at Los Alamos National Laboratory (subcontract number 75782-001-09), and by Los Alamos National Laboratory contract No. 75287-001-10.

References

- [1] J.F. Ziegler, J.P. Biersack, U. Littmark, *The Stopping and Range of Ions in Solids*, Pergamon Press, New York, 1985.
- [2] W. Eckstein, *Computer Simulation of Ion-Solid Interactions*, Springer-Verlag, New York, 1991.

- [3] K.M. Beardmore, N. Grønbech-Jensen, Efficient molecular dynamics scheme for the calculation of dopant profiles due to ion implantation, *Physics Review E* 57 (6) (1998) 7278–7287.
- [4] B. Jeon, N. Grønbech-Jensen, Efficient parallel algorithm for statistical ion track simulations in crystalline materials, *Computer Physics Communications* 180 (2) (2009) 231–237.
- [5] H. Kleykamp, The chemical state of the fission products in oxide fuels, *Journal of Nuclear Materials* 131 (2–3) (1985) 221–246.
- [6] J.R. Matthews, Technological problems and the future of research on the basic properties of actinide oxides, *Journal of the Chemical Society, Faraday Transactions 2: Molecular and Chemical Physics* 83 (7) (1987) 1273–1285.
- [7] J. Gittus, J. Matthews, P. Potter, Safety aspects of fuel behaviour during faults and accidents in pressurised water reactors and in liquid sodium cooled fast breeder reactors, *Journal of Nuclear Materials* 166 (1–2) (1989) 132–159.
- [8] M. Saïdy, W.H. Hocking, J.F. Mouris, P. Garcia, G. Carlot, B. Pasquet, Thermal diffusion of iodine in UO_2 and UO_{2+x} , *Journal of Nuclear Materials* 372 (2008) 405–415.
- [9] V.A. Elteckov, D.S. Karpuzov, Y.V. Martynenko, V.E. Yurasova, Computer studies of b^+ ion penetration into Si single crystal, in: *Atomic Collision Phenomena in Solids*, North-Holland, Amsterdam, 1969, pp. 657–662.
- [10] W. Brandt, M. Kitagawa, Effective stopping-power charges of swift ions in condensed matter, *Physical Review B* 25 (9) (1982) 5631–5637.
- [11] D. Cai, N. Grønbech-Jensen, C.M. Snell, K.M. Beardmore, Phenomenological electronic stopping-power model for molecular dynamics and monte carlo simulation of ion implantation into silicon, *Physics Review B* 54 (23) (1996) 17147–17157.
- [12] K. Nordlund, Molecular dynamics simulation of ion ranges in the 1–100 keV energy range, *Computational Materials Science* 3 (4) (1995) 448–456.
- [13] D. Cai, C.M. Snell, K.M. Beardmore, N. Grønbech-Jensen, Simulation of phosphorus implantation into silicon with a single-parameter electronic stopping power model, *International Journal of Modern Physics C* 9 (1998) 459–470.
- [14] K.M. Beardmore, N. Grønbech-Jensen, An efficient molecular dynamics scheme for predicting dopant implant profiles in semiconductors, *Nuclear Instruments and Methods in Physics Research Section B: Beam Interactions with Materials and Atoms* 153 (1999) 391–397.
- [15] J.F. Ziegler, J.P. Biersack, M.D. Ziegler, SRIM: The Stopping and Range of Ions in matter, SRIM Co., 2008. URL: <<http://www.SRIM.org>>.